Supplementary Information (SI) for Energy & Environmental Science.


# High triboelectrification and charge collection efficiency of direct current triboelectric nanogenerator achieved by tri-synergistic enhancement strategy

Shuyan Xu‡ [a], Jian Wang‡*[a], Chuncai Shan[a], Kaixian Li[a], Huiyuan Wu[a], Gui Li[a], Shaoke Fu[a], Qionghua Zhao[a], Yi Xi*[a] and Chenguo Hu*[a]

[1] Department of Applied Physics, Chongqing Key Laboratory of Soft Condensed Matter Physics and Smart Materials, Chongqing University, Chongqing 400044, P.R. China

[‡]S. Xu and J. Wang contributed equally to this work

Corresponding author email: iair_wangjian@cqu.edu.cn (J Wang), yxi6@cqu.edu.cn (Y Xi), hucg@cqu.edu.cn (C Hu)

**Supplementary Figure 1:** Photographs of corona discharge of TDD-TENGs with different units.

**Supplementary Figure 2:** The Output characteristics of dielectric materials with negative charge.

**Supplementary Figure 3:** The Output characteristics of dielectric materials with positive charge.

**Supplementary Figure 4:** The Output characteristics of 1-unit TDD-TENG slider with different stator.

**Supplementary Figure 5:** The Output characteristics of single PTFE slider and 1-unit TDD-TENG with different thickness of PTFE.

**Supplementary Figure 6:** The Output characteristics of 1-unit slider of TDD-TENG at different motion speed.

**Supplementary Figure 7:** SEM images of PU foam with different thickness.

**Supplementary Figure 8:** EDS mapping of PU foam after friction with PTFE.

**Supplementary Figure 9:** The output characteristics of 1-unit slider with same material.

**Supplementary Figure 10:** The output characteristics of 1-unit PTFE/X slider with and without PTFE pre-friction.

**Supplementary Figure 11:** The output characteristics of 1-unit X/PA slider with and without PTFE pre-friction.

**Supplementary Figure 12:** The Output charge comparation of 1-unit slider of PTFE/X and X/PA with and without PTFE pretreatment.

**Supplementary Figure 13:** SEM images of PU foam with spontaneously introduced PTFE and externally added PTFE power.

**Supplementary Figure 14:** Photos of PU with spontaneously introduced powder and externally added powder.

**Supplementary Figure 15:** The output characteristics of single PTFE and PA slider rubbed with PU coated excessive PTFE power.

**Supplementary Figure 16:** The output comparation of 1-unit slider of PTFE/PA with externally addation of different mass of PTFE power.

**Supplementary Figure 17:** Morphology of PTFE film after friction with PU.

**Supplementary Figure 18:** Morphology of PA film after 30 minutes friction with thickness of 20 μm.

**Supplementary Figure 19:** Photos of TDD-TENG sliders with different units of PTFE/PA.

**Supplementary Figure 20:** The Output characteristics of TDD-TENG with different units of PTFE/PA without preatment of PTFE.

**Supplementary Figure 21:** The output characteristics of 4-unit TDD-TENG at different motion speed with pretreatment of PTFE.

**Supplementary Figure 22:** The output characteristics of traditional binary DC-TENG with blank areas in different units with/without pretreatment of PTFE.

**Supplementary Figure 23:** The output characteristics of TDD-TENG with different units at different load resisitance.

**Supplementary Figure 24:** The output power of TDD-TENG with different units at different load resisitance.

**Supplementary Figure 25:** The leakage current of PU foam at different voltages with different thickness.

**Supplementary Figure 26:** The mechanism of DC-output on bottom electrode.

**Supplementary Figure 27:** The discharge images of bottom electrode.

**Supplementary Figure 28:** The output characteristics on unilateral and bilateral bottom electrode with at different unit on slider.

**Supplementary Figure 29:** Photograph of rotary TDD-TENG with different unit.

**Supplementary Figure 30:** The output characteristics of rotary TDD-TENG with different unit.

**Supplementary Figure 31:** The comparation of different rotary TDD-TENG with/without pretreatment of PTFE.

**Supplementary Figure 32:** Crest factor comparation of different units' rotary TDD-TENG with/without PTFE trearment.

**Supplementary Figure 33:** DC output on bottom electrodes of 3-unit TDD-TENG at rotary speed of 5rpm.

**Supplementary Note S1.** The calculation process of average power density of TDD-TENG.

**Supplementary Note S2.** The calculation process of maximum charge density of TDD-TENG.

**Supplementary Table S1.** Relevant data for calculating $I_{RMS}$ at the optimal matching impedance of sliding TDD-TENG.

**Supplementary Table S2.** Relevant data for calculating the maxium average power density of sliding TDD-TENG.

**Supplementary Table S3.** $I_{RMS}$ current and crest factor of TDD-TENG with different output units.

**Supplementary Table S4.** Relevant data for maximum charge density of TDD-TENG.

**Supplementary Table S5.** Relevant data for calculating average power density of rotary TDD-TENG.

**Supplementary Table S6.** Comparison of charge density and average power density of DC-TENG.

**Supplementary Video S1.** TDD-TENG for powering a buzzer.

**Supplementary Video S2.** A flood detector driven by TDD-TENG.

**Supplementary Video S3.** 74 hygrothermographs driven by the TDD-TENG.

**Supplementary Video S4.** 6 LED bulbs with power of 12W driven by the TDD-TENG.

**Supplementary Video S5.** 12 LED bulbs driven by TDD-TENG.

**Supplementary Video S6.** 4640 green LEDs illuminated by TDD-TENG.

**Supplementary Video S7.** The UV discharg tube illuminated by TDD-TENG.

**Supplementary Video S8.** 7 serise connected UV discharge tubes sterilize samples of trace water.

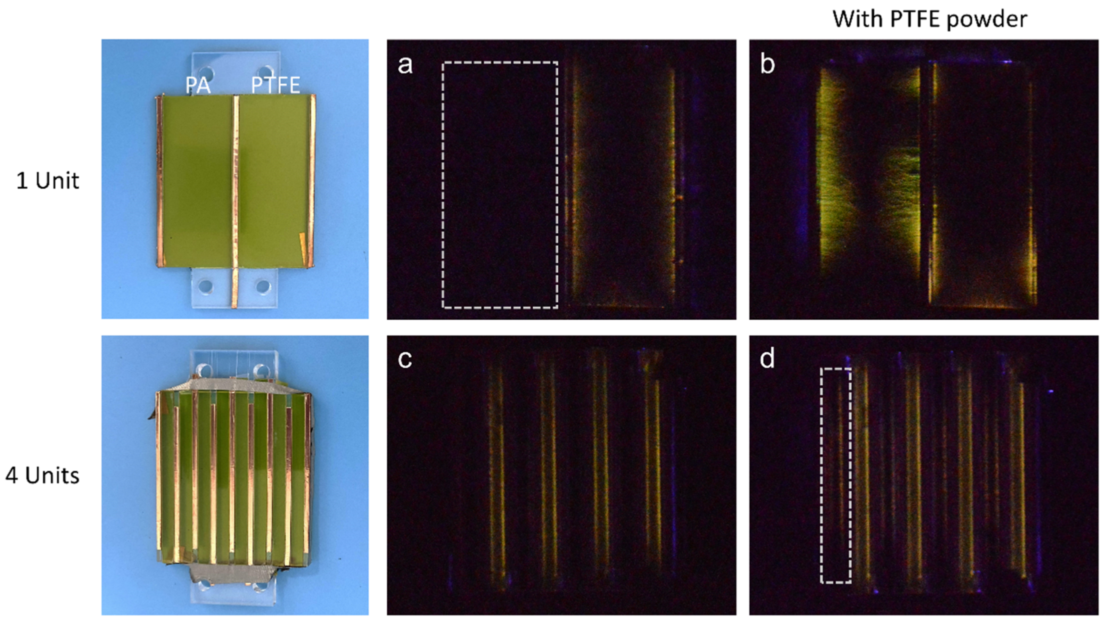


**Figure S1.** Photographs of corona discharge of TDD-TENGs. a) Corona discharge photo of 1-unit TDD-TENG without PTFE powder treatment. b) Corona discharge photo of 1-unit TDD-TENG with PTFE powder treatment. c) Corona discharge photo of 4-unit TDD-TENG without PTFE powder treatment. d) Corona discharge photo of 4-unit TDD-TENG with PTFE powder treatment.

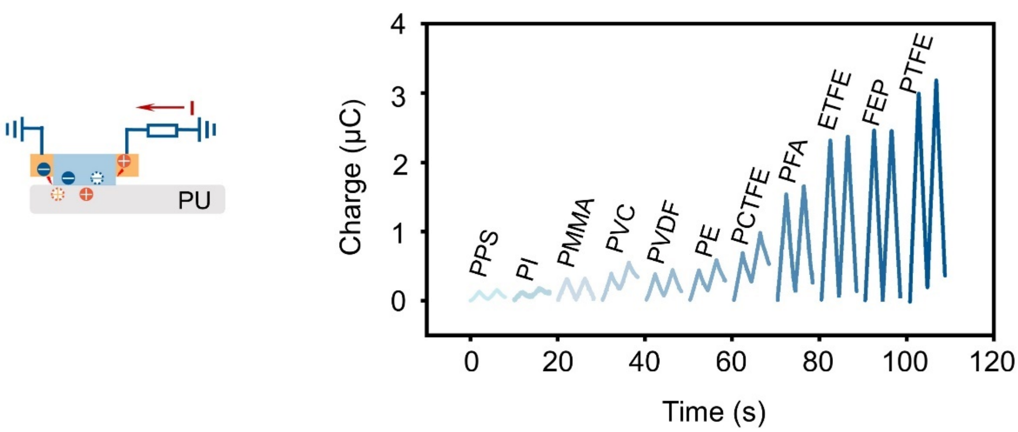


**Figure S2.** Output charge of dielectric materials with negative charge friction with PU.

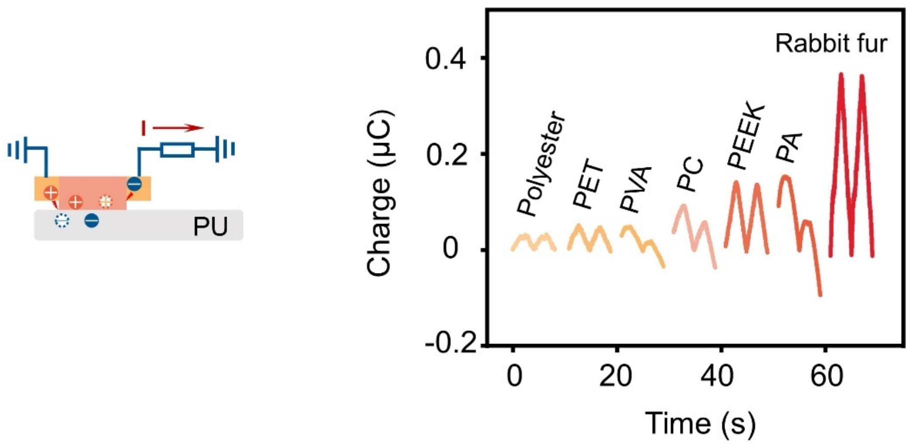


**Figure S3.** Output charge of dielectric materials with positive charge friction with PU.

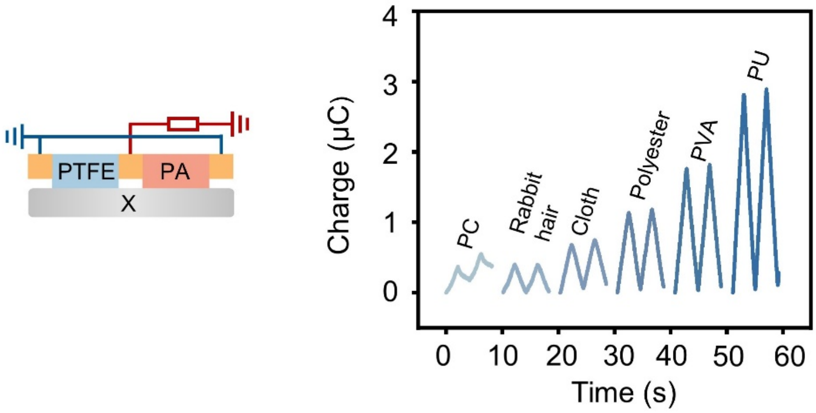


**Figure S4.** Output charge of 1-unit TDD-TENG slider with different stator.

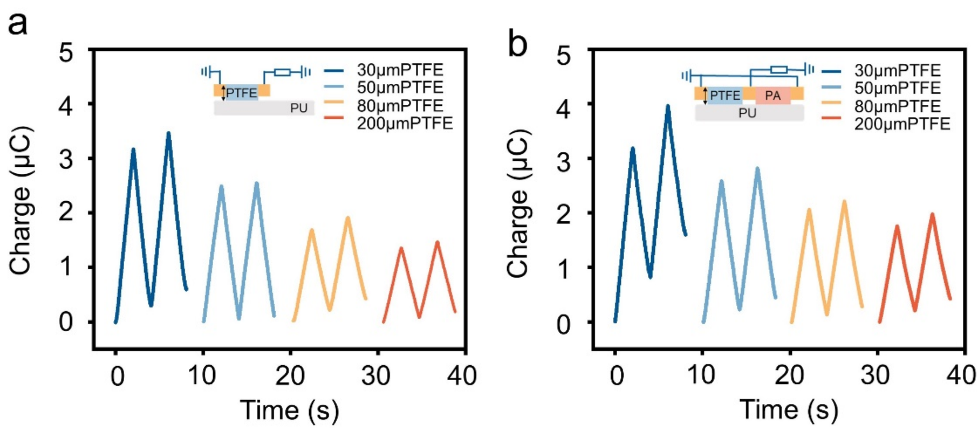


**Figure S5.** Output charge of a) single PTFE slider and b) 1-unit TDD-TENG with different thickness of PTFE.

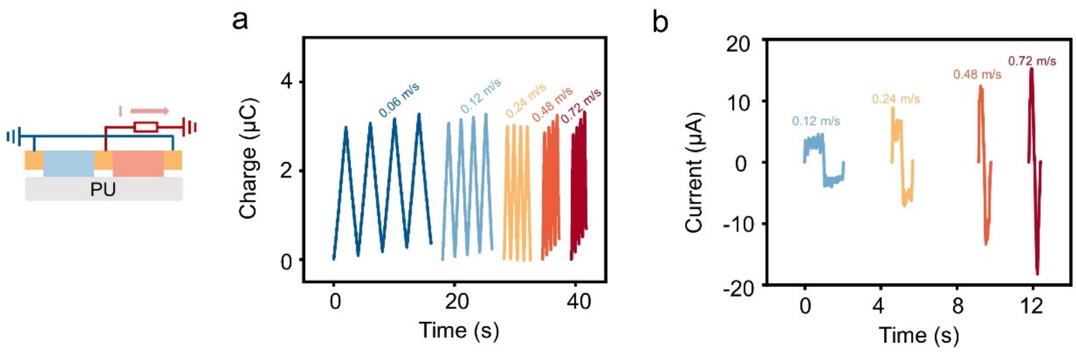


**Figure S6.** Output of 1-unit slider of TDD-TENG at different motion speed. a) Output charge and b) Output current of 1-unit TDD-TENG at different motion speed.

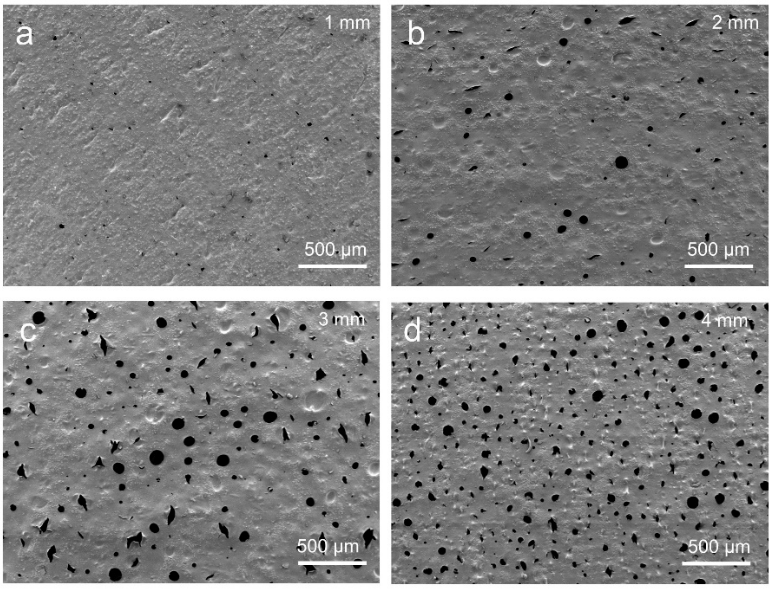


**Figure S7.** Scanning electron microscopy (SEM) images of PU foam with different thickness.

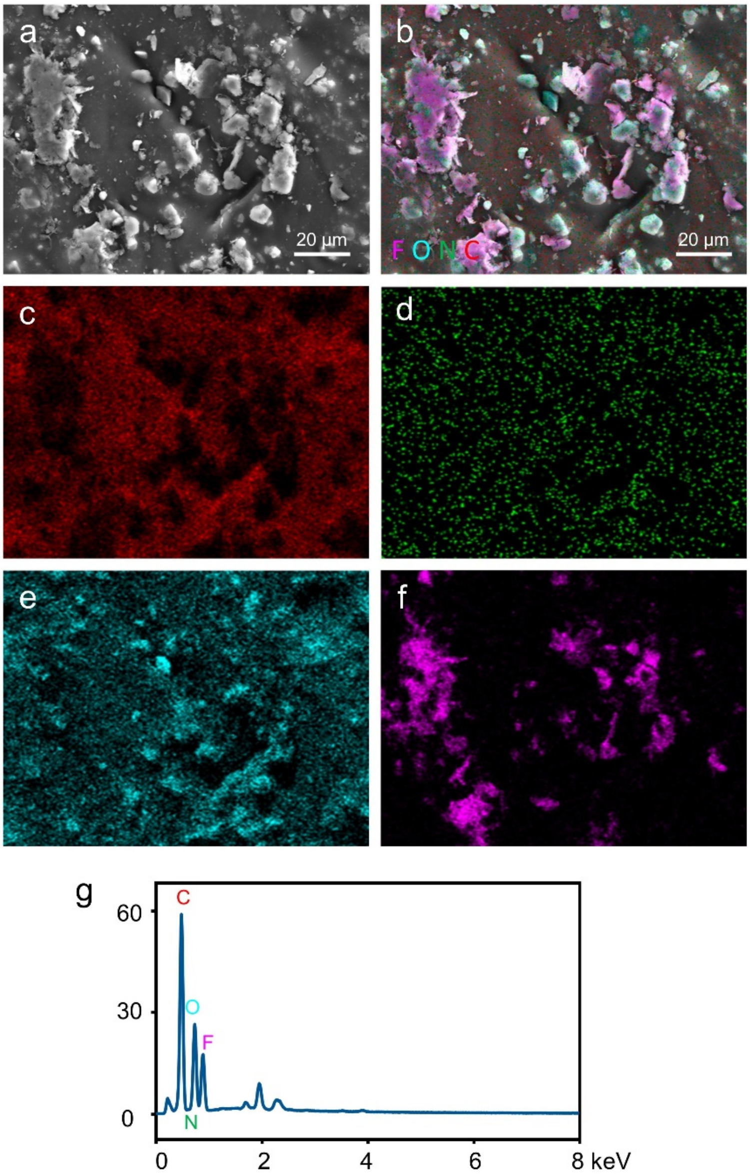


h

| Element | Wt % | Wt % Sigma | At % |
|---|---|---|---|
| C | 56.14 | 0.32 | 64.43 |
| N | 1.35 | 0.47 | 1.32 |
| O | 24.98 | 0.20 | 21.52 |
| F | 17.53 | 0.17 | 12.72 |
| Total | 100.00 | | 100.00 |

**Figure S8.** EDS mapping of PU foam after friction with PTFE.

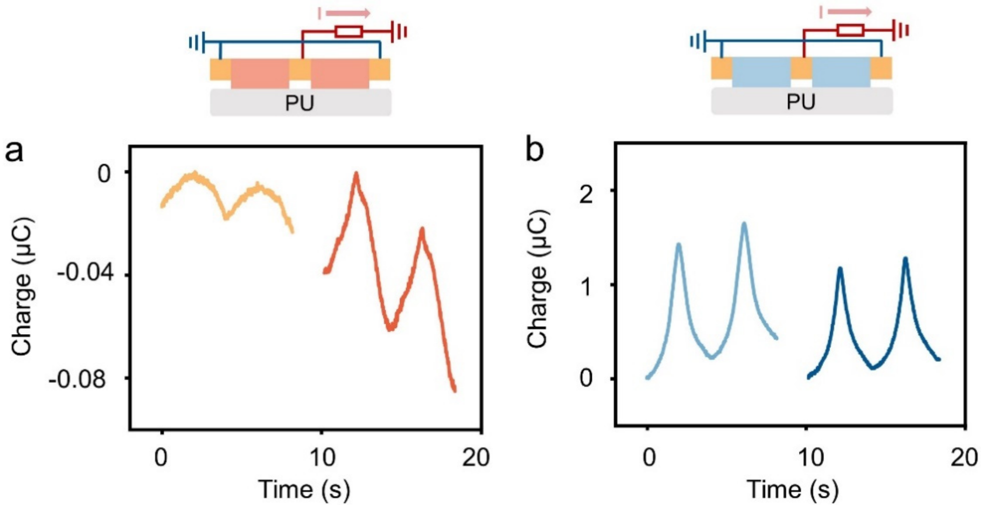


**Figure S9.** Output charge of 1-unit slider with same material. a) Output charge of 1-unit slider of PA b) Output charge of 1-unit slider of PTFE.

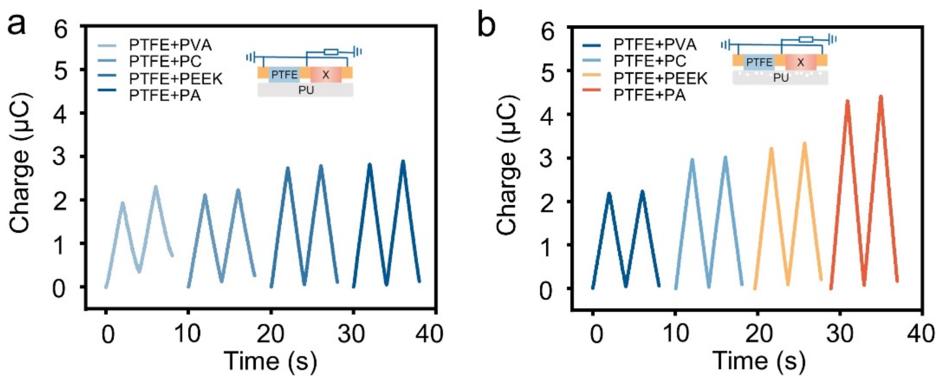


**Figure S10.** Output charge comparation of 1-unit slider of PTFE/X with and without PTFE pre-friction. a) Output charge of 1-unit slider of PTFE/X without PTFE pretreatment b) Output charge of 1-unit slider of PTFE/X with PTFE pretreatment

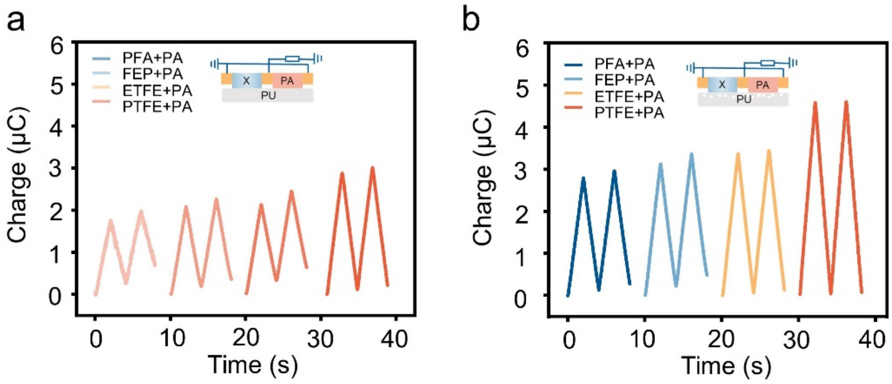


**Figure S11.** Output charge comparation of 1-unit slider of X/PA with and without PTFE pre-friction. a) Output charge of 1-unit slider of X/PA without PTFE pretreatment b) Output charge of 1-unit slider of X/PA with PTFE pretreatment

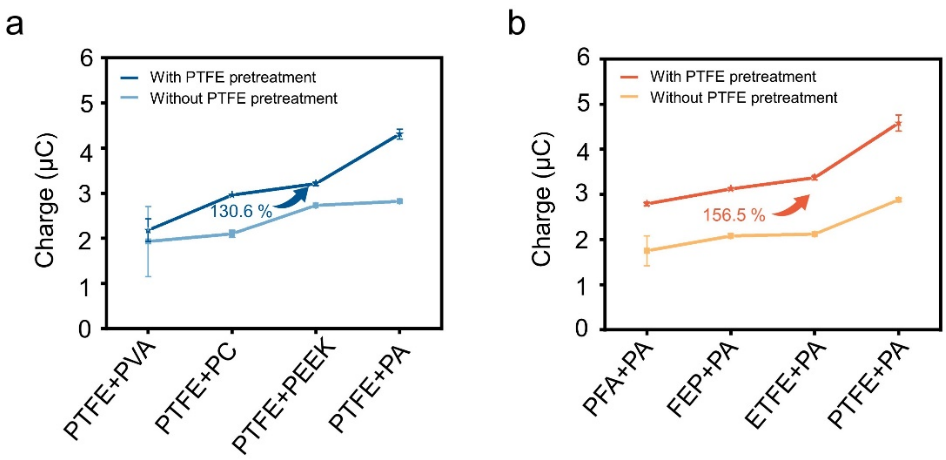


**Figure S12.** Output charge comparation of 1-unit slider of PTFE/X and X/PA with and without PTFE pretreatment. a) Output charge of 1-unit slider of PTFE/X with/without PTFE pretreatment b) Output charge of 1-unit slider of X/PA with PTFE pretreatment

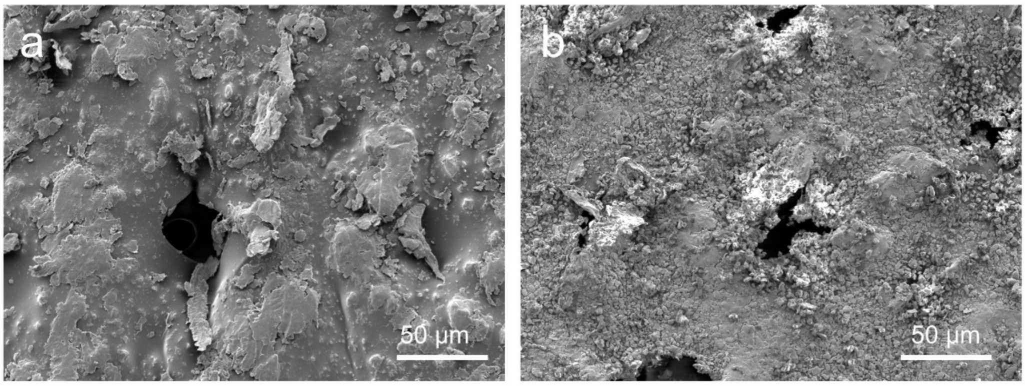


**Figure S13.** Scanning electron microscopy (SEM) images of PU foam with spontaneously introduced PTFE and externally added PTFE power with size of 10 μm.

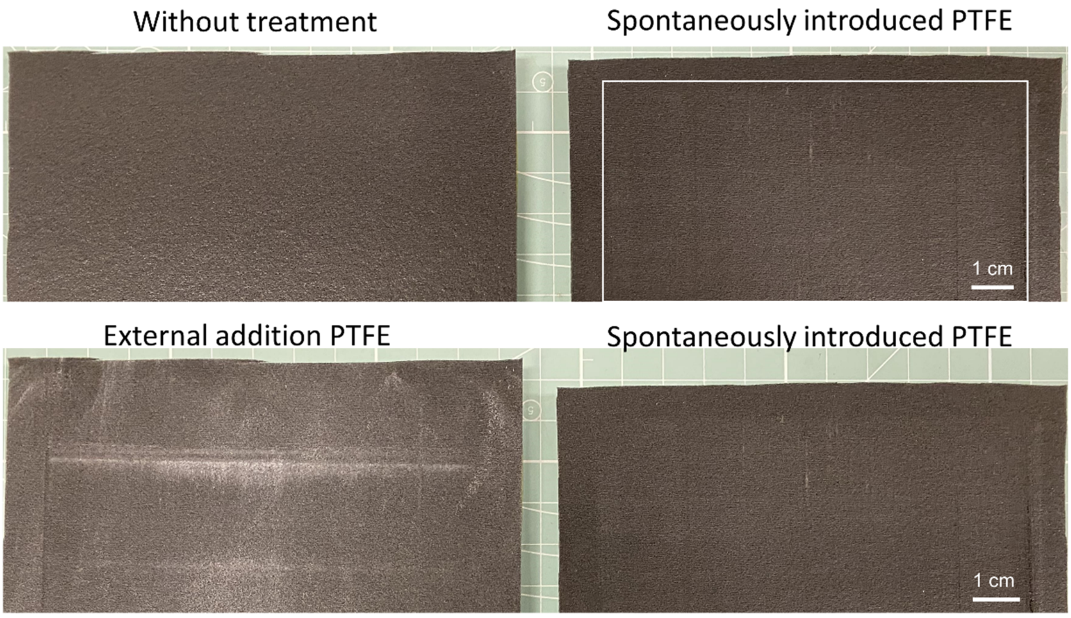


**Figure S14.** Photos of PU with spontaneously introduced powder and externally added powder.

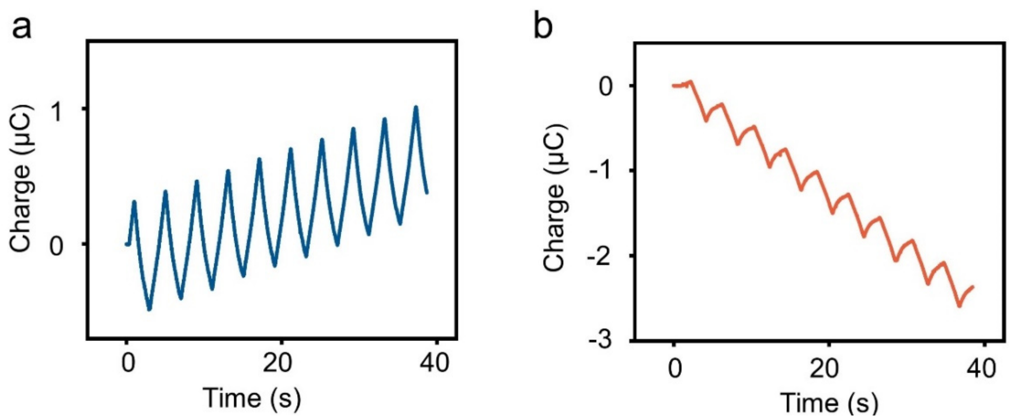


**Figure S15.** Output charge of single a) PTFE and b) PA slider rubbed with PU coated excessive PTFE power.

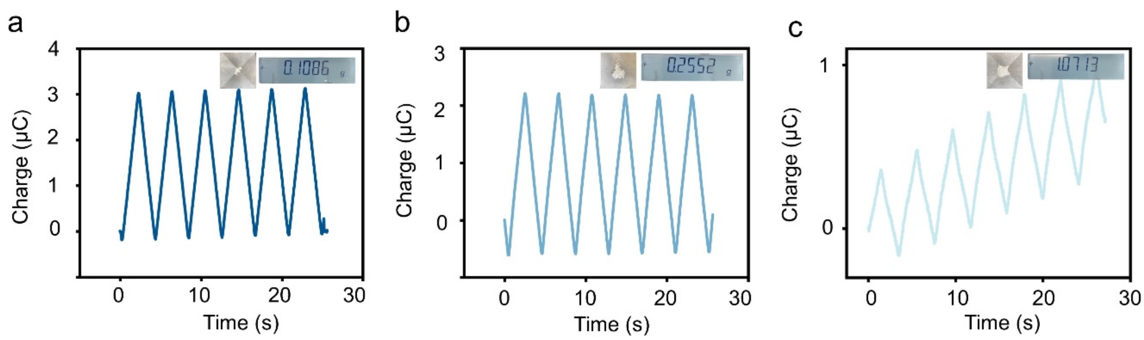


**Figure S16.** Output charge comparation of 1-unit slider of PTFE/PA with externally addation of different mass of PTFE power.

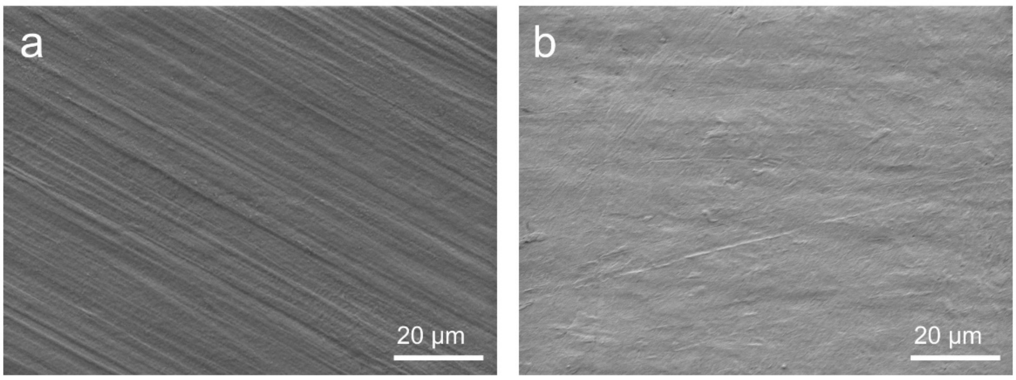


**Figure S17.** Morphology of PTFE film after 30 minutes of friction with thickness of 20 μm.

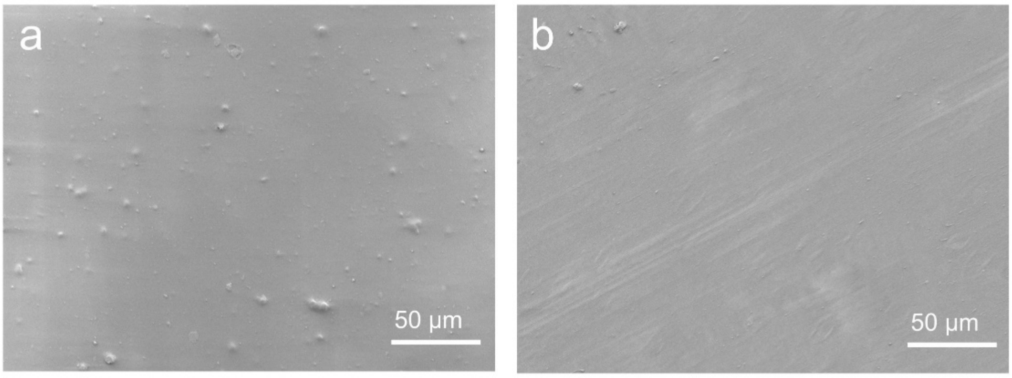


**Figure S18.** Morphology of PA film after 30 minutes friction with thickness of 20 μm.

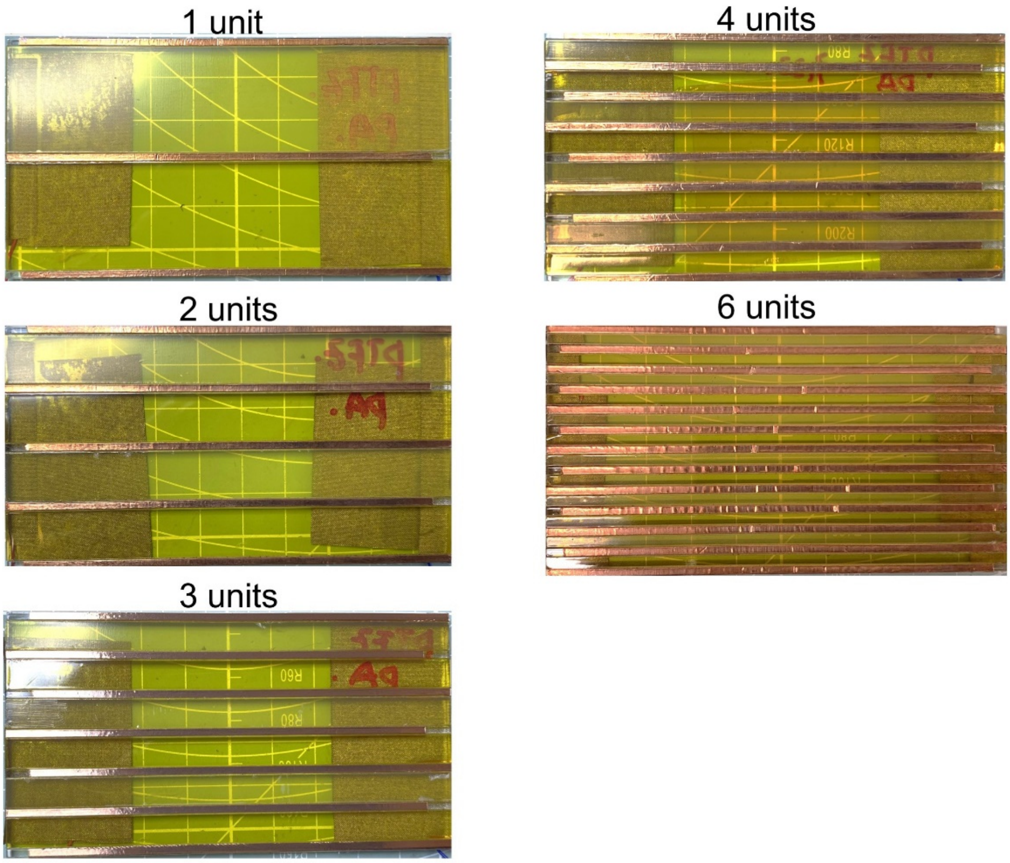


**Figure S19.** TDD-TENG sliders with different units of PTFE/PA.

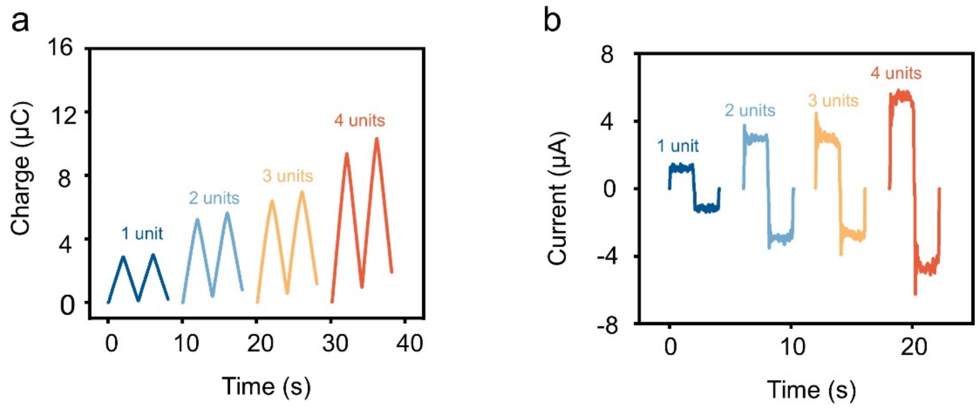


**Figure S20.** Output a)charge and b)current of TDD-TENG with different units of PTFE/PA without preatment of PTFE.

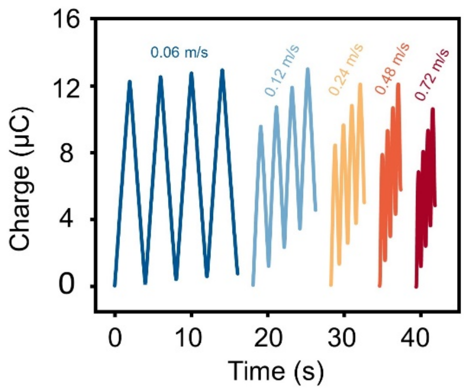


**Figure S21.** The output charge of 4-unit TDD-TENG at different motion speed with pretreatment of PTFE.

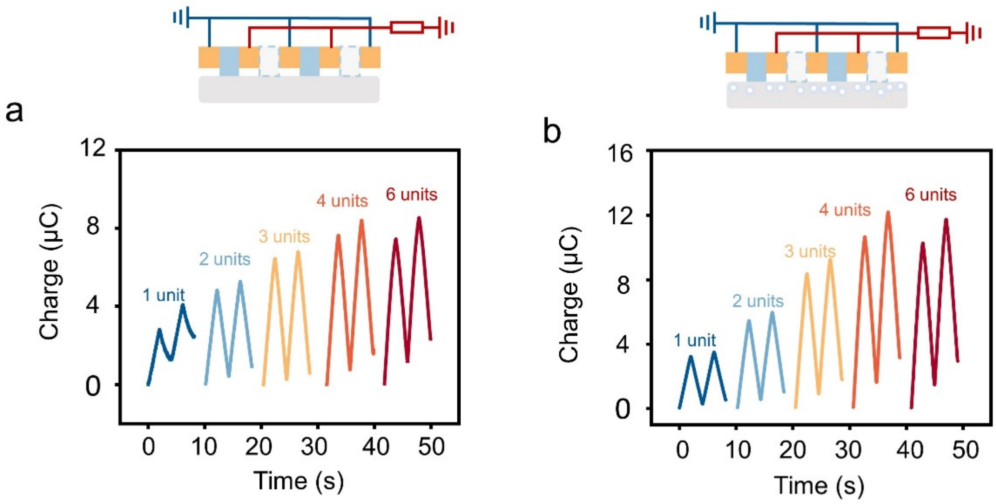


**Figure S22.** The output charge of traditional binary DC-TENG with blank areas in different units with/without pretreatment of PTFE.

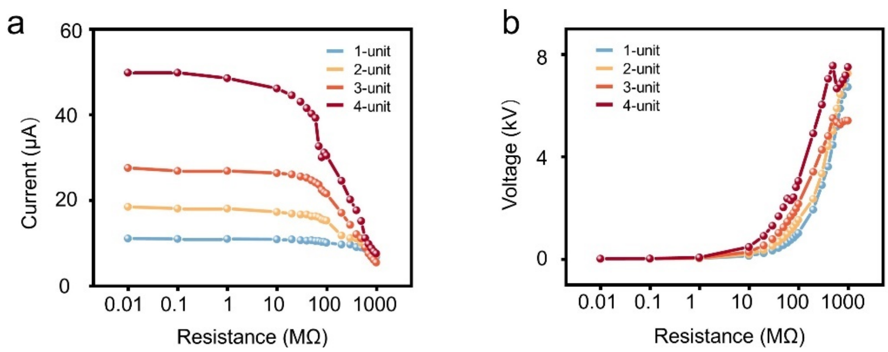


**Figure S23.** The output a) current and b) voltage of sliding TDD-TENG with different units at load resisitances from 0.01MΩ to 1GΩ with pretreatment of PTFE at motion speed of 0.72 m $s^{-1}$.

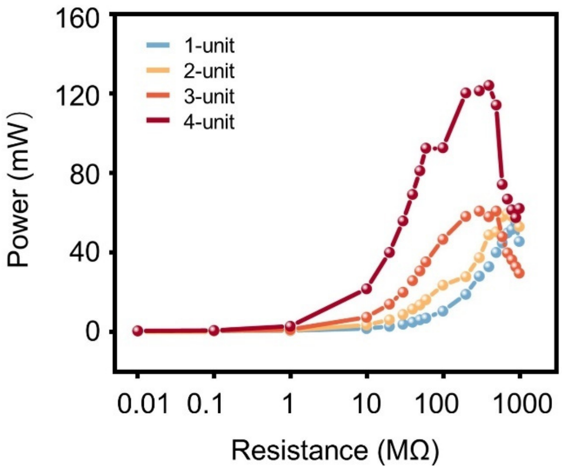


**Figure S24.** The output power of sliding TDD-TENG with different units at load resisitances from 0.01 MΩ to 1 GΩ with pretreatment of PTFE at motion speed of 0.72 m $s^{-1}$.

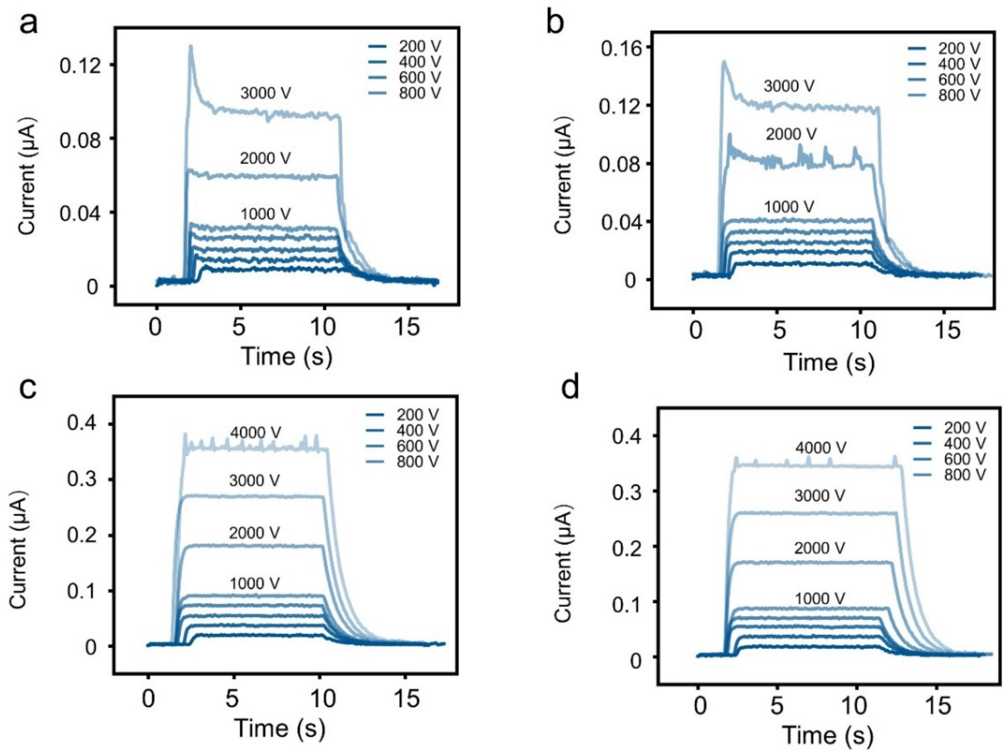


**Figure S25.** The leakage current of PU foam at different voltages (200-3000 V) with thickness of 2 mm, 3 mm, 4 mm, 5 mm.

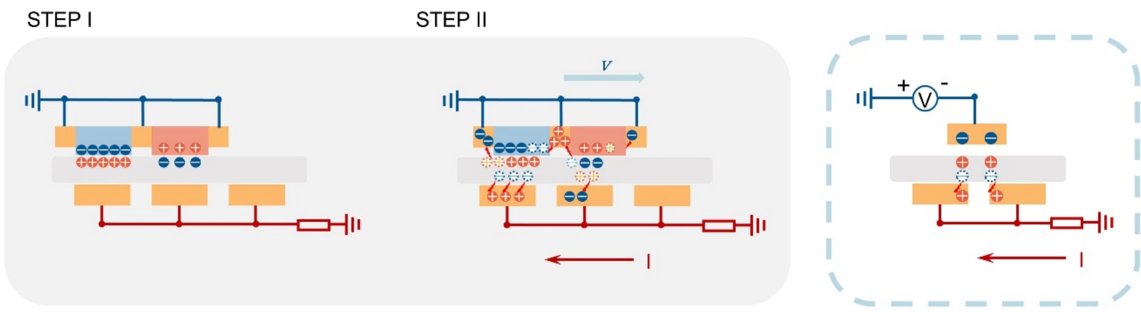


**Figure S26.** The mechanism of DC-output on bottom electrode.

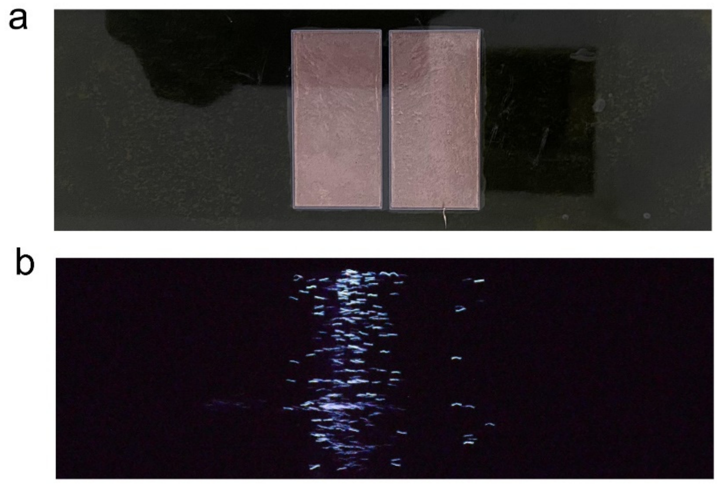


**Figure S27.** The discharge images of bottom electrodes. a) The photograph of the back of stator with a pair of bottom electrodes in light. b) The photograph of discharge on the back of stator in dark.

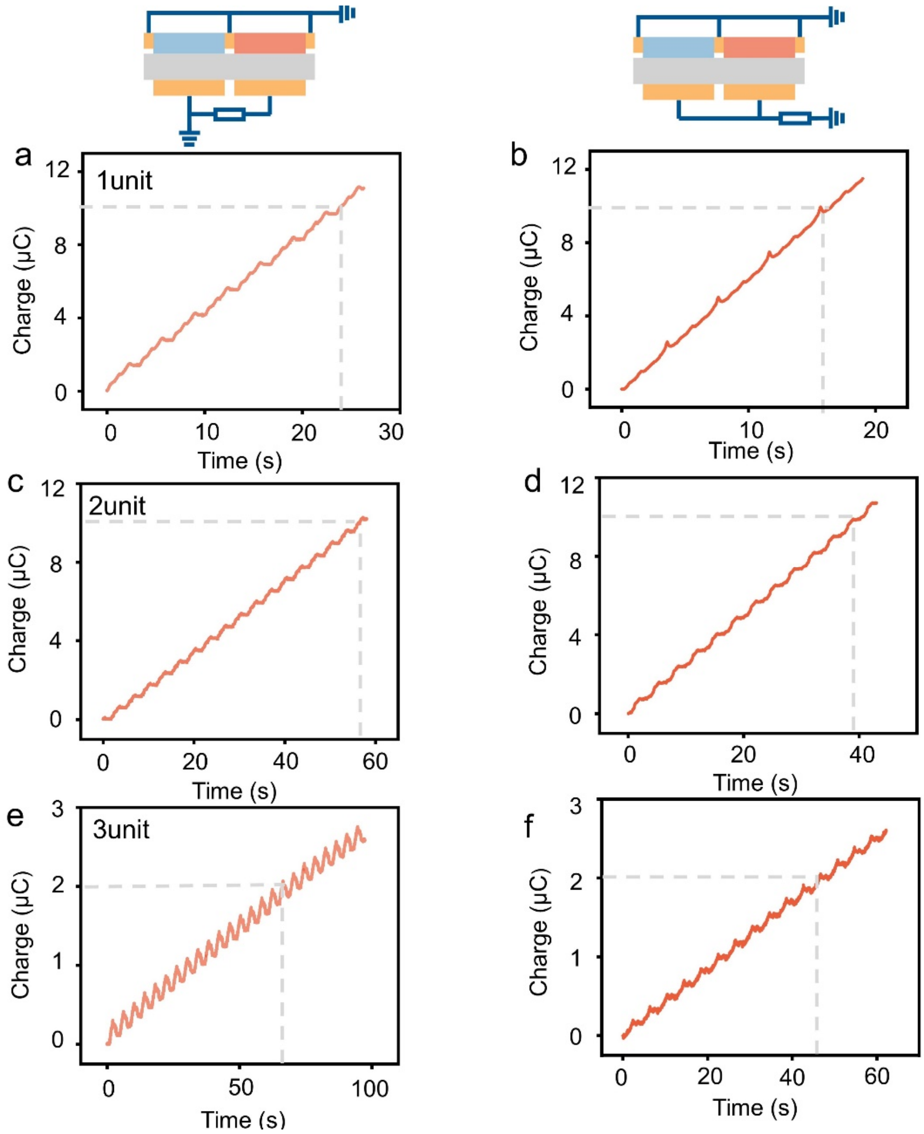


**Figure S28.** The output charge on unilateral and bilateral bottom electrode with at different unit on slider.

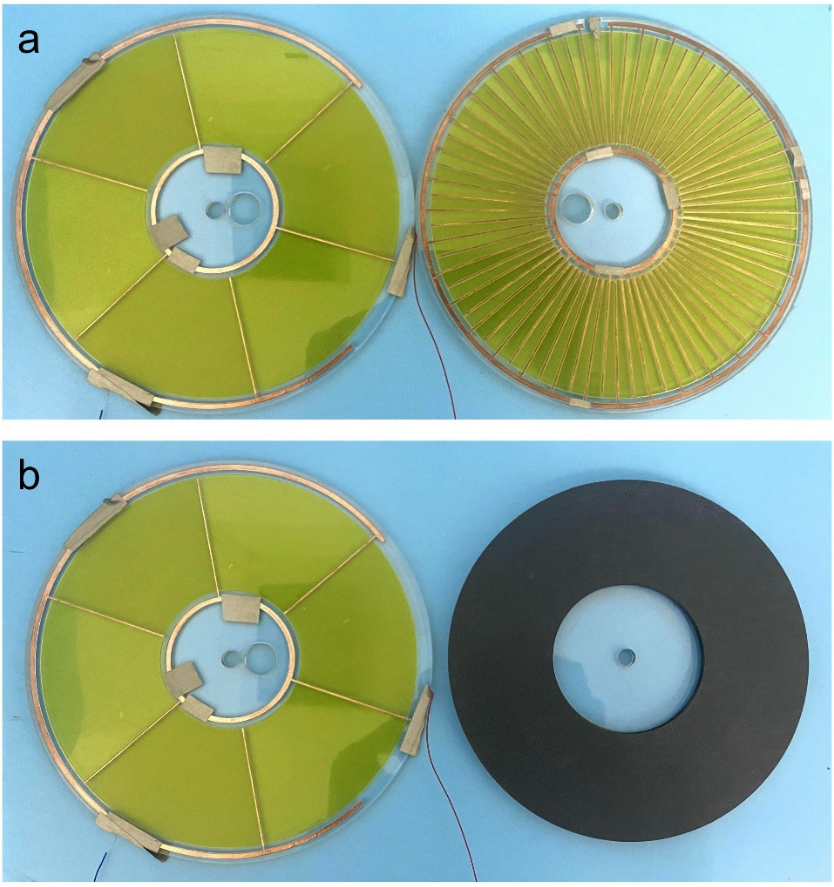


**Figure S29.** Photograph of rotary TDD-TENG with different unit.

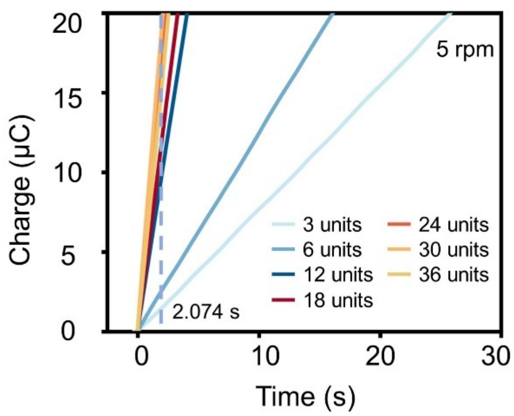


**Figure S30.** The output charge of rotary TDD-TENG with different unit at speed of 5 rpm.

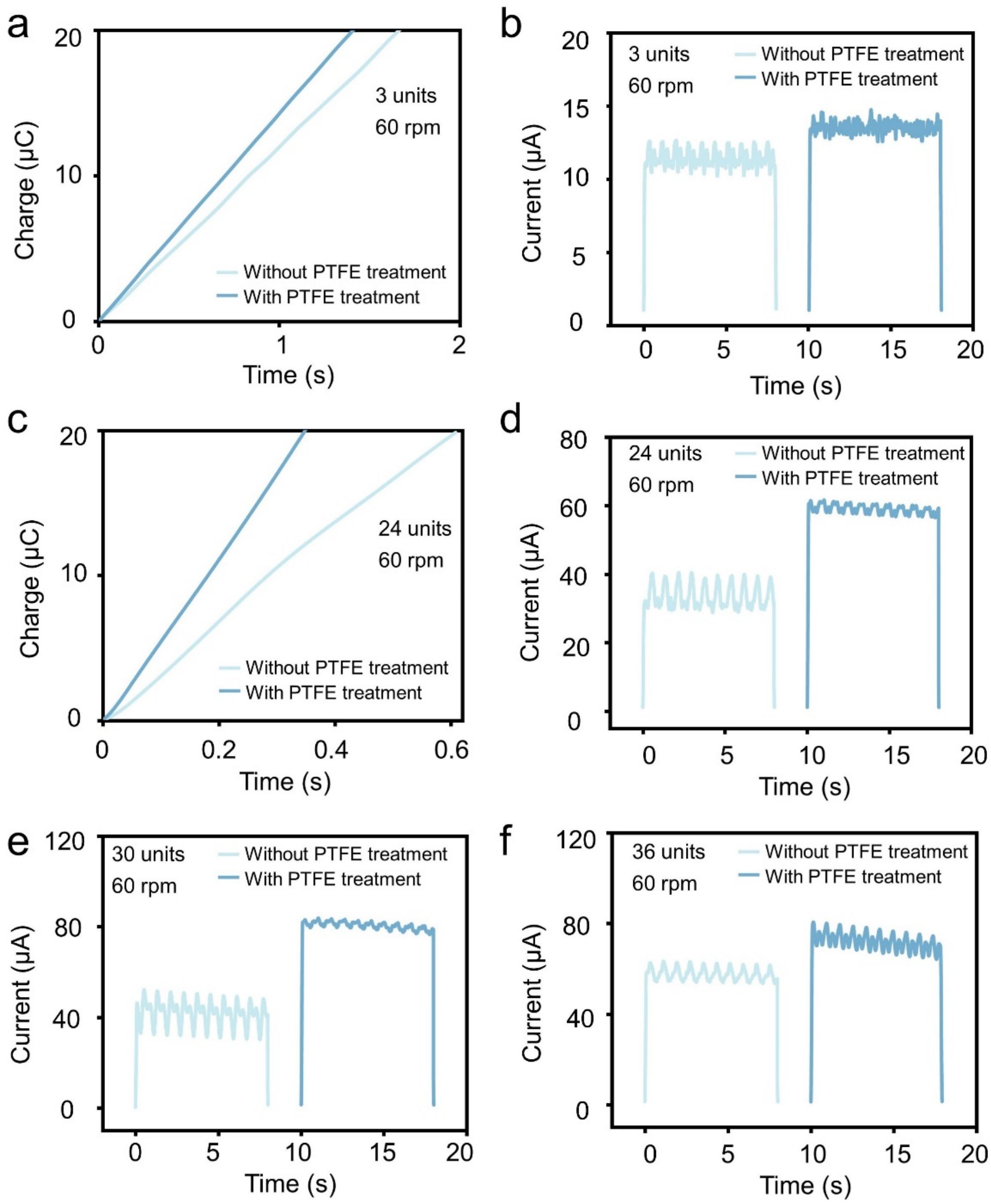


**Figure S31.** The comparation of output charge and current of different units' rotary TDD-TENG with/without pretreatment of PTFE.

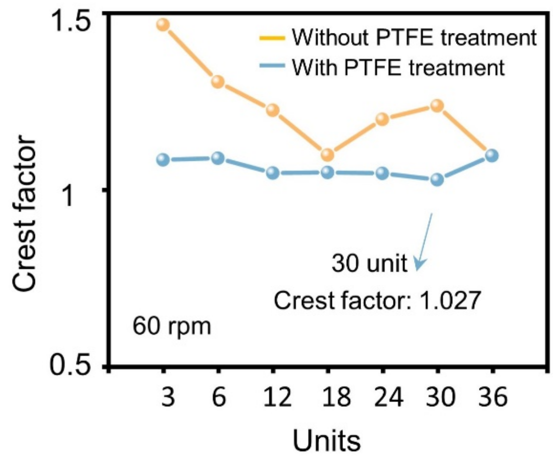


**Figure S32.** Crest factor comparation of different units' rotary TDD-TENG with/without PTFE treatment.

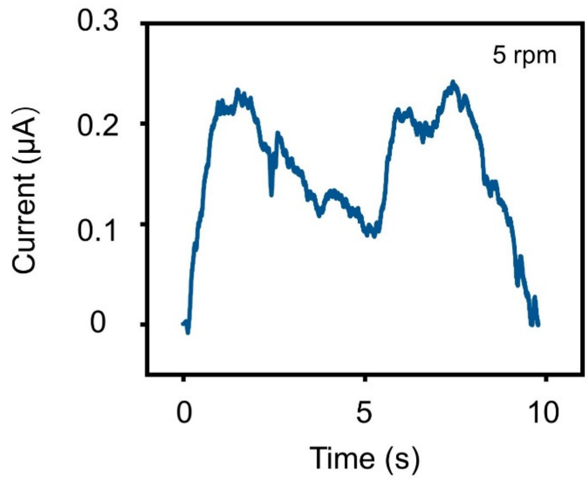


**Figure S33.** DC output on bottom electrodes of 3-unit TDD-TENG at rotary speed of 5 rpm.

**Supplementary Note S1.** The calculation process of average power density of TDD-TENG.

The average power density is an important indicator for evaluating the output performance of TENG. The calculation method for the average power density in this work is as follows: Firstly, calculate the RMS current under the optimal matching impedance using Origin Lab software, with the following formula

$$I_{RMS} = \sqrt{\frac{1}{n}\sum_{t=1}^{n} I_t^2}$$

Among them, in sliding mode, $n$ is the time taken to slide a distance of 120 mm, in rotary mode, $n$ is 4s, $I_t$ is the current value corresponding to each time point. Secondly, the average power density is calculated by

$$P_{er} = \frac{I_{RMS}^2 R}{S_f}$$

$R$ is the resistance at the best matching impedance point, $S_f$ is the total squre of PA and PTFE film on the slider.

**Supplementary Note S2.** The calculation process of maximum charge density of TDD-TENG.

The maximum charge density of rotatary TENG with different units were calculated as follow, by calculating the maximum transfer charge and friction area of PA and PTFE films on rotator for rotating TDD-TENGs with different units at a speed of 5 rpm, the maximum charge density can be obtained in following formula:

$$MCD = \frac{Q}{S_f}$$

$Q$ is the maximum transfer charge at the speed of 5 rpm, $S_f$ is the total square of PA and PTFE at the speed of 5 rpm. And the corresponding data are shown in Table S2.

**Supplementary Table S1.** Relevant data for calculating $I_{RMS}$ at the optimal matching impedance of sliding TDD-TENG.

| Unit | $\sum_{t=1}^{n} I_t^2$ | $t_1$ | $t_n$ | $\frac{1}{n}\sum_{t=1}^{n} I_t^2$ | $I_{RMS}$ (A) |
|---|---|---|---|---|---|
| 4-unit | 9.93E-11 | 22.4 | 23.001 | 1.65E-10 | 1.2857E-05 |

**Supplementary Table S2.** Relevant data for calculating the average power density of at the optimal matching impedance sliding TDD-TENG.

| Unit | $I_{RMS}$ (A) | $R$ (MΩ) | $P$ (W) | $S_f$ ($m^2$) | Average power density (W $m^{-2}$) |
|---|---|---|---|---|---|
| 4-unit | 1.2857E-05 | 400 MΩ | 0.066121198 | 0.0036 (0.054-0.002×9)× 0.1 | 18.36699945 |

**Supplementary Table S3.** $I_{RMS}$ and Crest Factor of TDD-TENG with different output units.

| Unit | Δt (s) | $\sum_{t=1}^{n} I_t^2$ (A) | $I_{RMS}$ (A) | $I_{peak}$ (A) | CF |
|---|---|---|---|---|---|
| 3 | 4.000 | 8.59E-11 | 4.63E-06 | 6.96E-06 | 1.502 |
| 3 (PTFE) | 3.999 | 7.36E-10 | 1.36E-05 | 1.47E-05 | 1.084 |
| 6 | 3.999 | 2.50E-10 | 7.91E-06 | 1.04E-05 | 1.315 |
| 6 (PTFE) | 3.999 | 1.23E-09 | 1.752E-05 | 1.90E-05 | 1.084 |
| 12 | 3.999 | 5.38E-09 | 3.668E-05 | 3.93E-05 | 1.071 |
| 12 (PTFE) | 3.999 | 7.72E-09 | 4.39E-05 | 4.60E-05 | 1.047 |
| 18 | 3.999 | 5.94E-09 | 3.85E-05 | 4.23E-05 | 1.097 |
| 18 (PTFE) | 3.999 | 1.21E-08 | 5.50E-05 | 5.77E-05 | 1.048 |
| 24 | 3.999 | 4.57E-09 | 3.38E-05 | 4.04 E-05 | 1.195 |
| 24 (PTFE) | 3.998 | 1.41E-08 | 5.94E-05 | 6.16 E-05 | 1.036 |
| 30 | 3.999 | 7.36E-09 | 4.29E-05 | 5.20E-05 | 1.212 |
| 30 (PTFE) | 3.998 | 2.65E-08 | 8.14E-05 | 8.37E-05 | 1.027 |
| 36 | 3.999 | 1.32E-8 | 5.76E-05 | 6.31E-05 | 1.096 |
| 36 (PTFE) | 3.998 | 2.16E-08 | 7.36E-05 | 8.06E-05 | 1.095 |

**Supplementary Table S4.** Relevant data for calculating maximum charge density of TDD-TENG.

| Unit | *t* (reach 20 μC at 5 rpm) (s) | Transfer Charge (μC $s^{-2}$) | $S_{total}$ ($mm^2$) | $S_f$ (at 5rpm) ($mm^2$ $s^{-2}$) | Maximum charge density (mC $m^{-2}$) |
|---|---|---|---|---|---|
| 3 | 26.585 | 0.752 | 18540 | 1545 | 0.487 |
| 3 (PTFE) | 25.834 | 0.774 | 18540 | 1545 | 0.501 |
| 6 | 17.75 | 1.127 | 18240 | 1520 | 0.741 |
| 6 (PTFE) | 16.127 | 1.240 | 18240 | 1520 | 0.816 |
| 12 | 7.22 | 2.770 | 17640 | 1470 | 1.884 |
| 12 (PTFE) | 4.094 | 4.885 | 17640 | 1470 | 3.323 |
| 18 | 4.96 | 4.032 | 17040 | 1420 | 2.839 |
| 18 (PTFE) | 3.317 | 6.030 | 17040 | 1420 | 4.246 |
| 24 | 2.974 | 6.725 | 16440 | 1370 | 4.909 |
| 24 (PTFE) | 2.341 | 8.543 | 16440 | 1370 | 6.236 |
| 30 | 2.122 | 9.425 | 15840 | 1320 | 7.140 |
| 30 (PTFE) | 2.074 | 9.643 | 15840 | 1320 | 7.305 |
| 36 | 2.329 | 8.587 | 15240 | 1270 | 6.761 |
| 36 (PTFE) | 2.167 | 9.229 | 15240 | 1270 | 7.267 |

**Supplementary Table S5.** Relevant data for calculating average power density of rotary TDD-TENG.

| Unit | $I_{RMS}$ (A) | *R* (MΩ) | *P* (W) | $S_f$ ($m^2$) | Average power density (W $m^{-2}$) |
|---|---|---|---|---|---|
| 30-unit (30 rpm) | 1.89 E-05 | 200 MΩ | 7.14E-02 | 0.66 | 1.08E+01 |

**Supplementary Table S6.** Comparison of charge density and average power density of DC-TENG.

| Ref | Article | Tribo-materials | AC/DC | Average power density (W m-2) |
|---|---|---|---|---|
| 1 | Zhang et.al (2014) Adv. Energy Mater | Al/PVC | DC | 0.025 |
| 2 | Zhang et.al (2024) Energy Environ. Sci | NC/PU | DC | 0.071 |
| 3 | Shan et.al (2021) Energy Environ. Sci | PA/Kapton | DC | 0.095 |
| 4 | Chen et.al (2022) Adv. Energy Mater | PTFE yarn | DC | 0.18 |
| 5 | Zhao et.al (2021) Nat. Commun | Cu/PVC | DC | 0.2 |
| 6 | Lei et.al (2020) Energy Environ. Sci | PA/Kapton/Cloth | DC | 0.24 |
| 7 | Zhang et.al (2023) Nat. Commun | Cu/PVC | DC | 0.24 |
| 8 | Liu et.al (2019) Sci. Adv | Cu/PTFE | DC | 0.35 |
| 9 | Zeng et.al (2022) Adv. Mater | PU/PTFE | DC | 0.398 $W\ m^{-2}\ Hz^{-1}$ |
| 10 | He et.al (2022) ACS Nano | PTFE/PA | DC | 0.89 |
| 11 | Qiao et.al (2021) Nona Energy | Cu/FEP | DC | 0.96 |
| 12 | Chen et.al (2021) Energy Environ. Sci | Rabbit fur/PTFE | DC | 1.11 |
| 13 | Li et.al (2022) Energy Environ. Sci | PVC/Cu | DC | 1.98 |
| 14 | Luo et.al (2018) Adv. Energy Mater | Al/FEP | DC | 2.03 |
| 15 | Gao et.al (2024) Nat. Commun | ETFE/PI | DC | 2.32 |
| 16 | Shan et.al (2022) Adv. Energy Mater | PTFE/PA | DC | 3 |
| 17 | Fu et.al (2022) Nano Micro Letters | FEP/Al/PA | DC | 3.1 |
| 18 | Du et.al (2022) Adv. Funct. Mater. | FEP/PA | DC | 4.2 |
| 19 | Liu et.al (2022) Small | Cu/PTFE | DC | 4.84 |

| | | | | |
|---|---|---|---|---|
| 20 | Ryu et.al (2018) Energy Environ. Sci | PTFE/MC Nylon | DC | 4.9 |
| 21 | Meng et.al (2022) Energy Environ. Sci | Al/PPy | DC | 5.4 |
| 22 | He et.al (2022) Adv. Energy Mater | PTFE/PA | DC | 5.74 W $m^{-2}$ $Hz^{-1}$ |
| 23 | Li et.al (2022) Energy Environ. Sci | PTFE/PA/PET | DC | 6.15 W $m^{-2}$ $Hz^{-1}$ |
| 24 | Sun et.al (2022) Energy Environ. Sci | PTFE/PMMA/Rubber | DC | 7.9 |
| 25 | Shan et.al (2022) Nano Energy | PTFE/Cloth | DC | 9.8 |
| 26 | Li et.al (2024) Energy Environ. Sci | PTFE/PU | DC | 9.98 |
| 27 | Shan et.al (2023) Adv. Funct. Mater. | PTFE/PI/PU | DC | 12.4 |
| | This work | PTFE/PA/PU | DC | 18.37 (Sliding) |

## Reference


1. C. Zhang, T. Zhou, W. Tang, C. Han, L. Zhang and Z. L. Wang, *Advanced Energy Materials*, 2014, **4**.
2. X. Zhang, D. Ren, H. Wu, J. Wang, X. Li, H. Yang, Q. Li, Q. Yang, J. Zhu and Y. Xi, *Energy & Environmental Science*, 2024, **17**, 4175-4186.
3. C. Shan, W. Liu, Z. Wang, X. Pu, W. He, Q. Tang, S. Fu, G. Li, L. Long, H. Guo, J. Sun, A. Liu and C. Hu, *Energy & Environmental Science*, 2021, **14**, 5395-5405.
4. R. Cheng, C. Ning, P. Chen, F. Sheng, C. Wei, Y. Zhang, X. Peng, K. Dong and Z. L. Wang, *Advanced Energy Materials*, 2022, **12**.
5. Z. Zhao, L. Zhou, S. Li, D. Liu, Y. Li, Y. Gao, Y. Liu, Y. Dai, J. Wang and Z. L. Wang, *Nat Commun*, 2021, **12**, 4686.
6. R. Lei, Y. Shi, Y. Ding, J. Nie, S. Li, F. Wang, H. Zhai, X. Chen and Z. L. Wang, *Energy & Environmental Science*, 2020, **13**, 2178-2190.
7. J. Zhang, Y. Gao, D. Liu, J. S. Zhao and J. Wang, *Nat Commun*, 2023, **14**, 3218.

8. X. Y. Di Liu, Hengyu Guo, Linglin Zhou, Xinyuan Li, Chunlei Zhang, Jie Wang, Zhong Lin Wang, *Sci. Adv*, 2019, **5**, eaav6437.
9. Q. Zeng, A. Chen, X. Zhang, Y. Luo, L. Tan and X. Wang, *Adv Mater*, 2023, **35**, e2208139.
10. L. He, C. Zhang, B. Zhang, O. Yang, W. Yuan, L. Zhou, Z. Zhao, Z. Wu, J. Wang and Z. L. Wang, *ACS Nano*, 2022, **16**, 6244-6254.
11. G. Qiao, J. Wang, X. Yu, R. Jia, T. Cheng and Z. L. Wang, *Nano Energy*, 2021, **79**.
12. P. Chen, J. An, R. Cheng, S. Shu, A. Berbille, T. Jiang and Z. L. Wang, *Energy & Environmental Science*, 2021, **14**, 4523-4532.
13. X. Li, C. Zhang, Y. Gao, Z. Zhao, Y. Hu, O. Yang, L. Liu, L. Zhou, J. Wang and Z. L. Wang, *Energy & Environmental Science*, 2022, **15**, 1334-1345.
14. J. Luo, L. Xu, W. Tang, T. Jiang, F. R. Fan, Y. Pang, L. Chen, Y. Zhang and Z. L. Wang, *Advanced Energy Materials*, 2018, **8**.
15. Y. Gao, L. He, D. Liu, J. Zhang, L. Zhou, Z. L. Wang and J. Wang, *Nat Commun*, 2024, **15**, 4167.
16. C. Shan, W. He, H. Wu, S. Fu, Q. Tang, Z. Wang, Y. Du, J. Wang, H. Guo and C. Hu, *Advanced Energy Materials*, 2022, **12**.
17. S. Fu, W. He, H. Wu, C. Shan, Y. Du, G. Li, P. Wang, H. Guo, J. Chen and C. Hu, *Nanomicro Lett*, 2022, **14**, 155.
18. Y. Du, S. Fu, C. Shan, H. Wu, W. He, J. Wang, H. Guo, G. Li, Z. Wang and C. Hu, *Advanced Functional Materials*, 2022, **32**.
19. L. Liu, Z. Zhao, Y. Li, X. Li, D. Liu, S. Li, Y. Gao, L. Zhou, J. Wang and Z. L. Wang, *Small*, 2022, **18**, e2201402.
20. H. Ryu, J. H. Lee, U. Khan, S. S. Kwak, R. Hinchet and S.-W. Kim, *Energy & Environmental Science*, 2018, **11**, 2057-2063.
21. J. Meng, C. Pan, L. Li, Z. H. Guo, F. Xu, L. Jia, Z. L. Wang and X. Pu, *Energy & Environmental Science*, 2022, **15**, 5159-5167.
22. W. He, C. Shan, H. Wu, S. Fu, Q. Li, G. Li, X. Zhang, Y. Du, J. Wang, X. Wang and C. Hu, *Advanced Energy Materials*, 2022, **12**.

23. Q. Li, S. Fu, X. Li, H. Chen, W. He, Q. Yang, X. Zhang, H. Yang, D. Ren and Y. Xi, *Energy & Environmental Science*, 2023, **16**, 3514-3525.

24. D.-J. Sun, W.-Z. Song, C.-L. Li, T. Chen, D.-S. Zhang, J. Zhang, S. Ramakrishna and Y.-Z. Long, *Nano Energy*, 2022, **101**.

25. C. Shan, W. He, H. Wu, S. Fu, G. Li, Y. Du, J. Wang, Q. Mu, H. Guo, B. Liu and C. Hu, *Nano Energy*, 2022, **104**.

26. K. Li, C. Shan, S. Fu, H. Wu, W. He, J. Wang, G. Li, Q. Mu, S. Du, Q. Zhao, C. Hu and H. Guo, *Energy & Environmental Science*, 2024, **17**, 580-590.

27. C. Shan, K. Li, H. Wu, S. Fu, A. Liu, J. Wang, X. Zhang, B. Liu, X. Wang and C. Hu, *Advanced Functional Materials*, 2023, **34**.